

# Polymer Chemistry

Accepted Manuscript



This is an *Accepted Manuscript*, which has been through the Royal Society of Chemistry peer review process and has been accepted for publication.

*Accepted Manuscripts* are published online shortly after acceptance, before technical editing, formatting and proof reading. Using this free service, authors can make their results available to the community, in citable form, before we publish the edited article. We will replace this *Accepted Manuscript* with the edited and formatted *Advance Article* as soon as it is available.

You can find more information about *Accepted Manuscripts* in the [Information for Authors](#).

Please note that technical editing may introduce minor changes to the text and/or graphics, which may alter content. The journal's standard [Terms & Conditions](#) and the [Ethical guidelines](#) still apply. In no event shall the Royal Society of Chemistry be held responsible for any errors or omissions in this *Accepted Manuscript* or any consequences arising from the use of any information it contains.

Cite this: DOI: 10.1039/c0xx00000x

www.rsc.org/xxxxxx

ARTICLE TYPE

## Solution Processible Hyperbranched Inverse-Vulcanized Polymers as New Cathode Materials in Li-S Batteries

Yangyang Wei<sup>a</sup>, Xiang Li<sup>b</sup>, Zhen Xu<sup>a</sup>, Haiyan Sun<sup>a</sup>, Yaochen Zheng<sup>a,c</sup>, Sipei Li<sup>a</sup>, Li Peng<sup>a</sup>, Zheng Li<sup>a</sup>, Zheng Liu<sup>a</sup>, Xiaozhen Hu<sup>a</sup>, Xiaoli Zhao<sup>a</sup>, Tieqi Huang<sup>a</sup>, Bo Zhao<sup>a</sup>, Jiabin Xi<sup>a</sup>, Chao Gao<sup>\*a</sup> and Mingxia Gao<sup>\*b</sup>

Received (in XXX, XXX) Xth XXXXXXXXXX 20XX, Accepted Xth XXXXXXXXXX 20XX

DOI: 10.1039/b000000x

Soluble inverse-vulcanized hyperbranched polymers (SIVHPs) were synthesized *via* radical ring-opening polymerization (RROP) of sulfur (S<sub>8</sub>) with 1,3-diisopropenylbenzene (DIB) in solution. Benefited from their branched molecular architecture and crosslinking-free merit, SIVHPs presented excellent solubility in polar organic solvents with an ultrahigh concentration of 400 mg mL<sup>-1</sup>. After end-capping by sequential click chemistry of thiol-ene and Menschutkin-quaternization reactions, we obtained water soluble SIVHPs for the first time. The sulfur-rich SIVHPs were employed as solution processible cathode-active materials for Li-S batteries, by facile fluid infiltration into conductive frameworks of graphene-based ultralight aerogels (GUAs). The SIVHPs-based cells showed high initial specific capacities of 1247.6 mA h g<sup>-1</sup>, good cyclability of 694.0 mA h g<sup>-1</sup> after 90 cycles. The cells also demonstrated an excellent rate capability and a considerable depression of shuttle effect with stable coulombic efficiency of around 100%. The electrochemical performance of SIVHP in Li-S batteries overwhelmed the case of neat sulfur, due to the chemical fixation of sulfur. The combination of high solubility, structure flexibility, and superior electrochemical performance opens a door for the promising application of SIVHPs.

### Introduction

Hyperbranched polymers (HPs) have attracted wide attention due to their distinctive chemical and physical properties, which are derived from their unique three-dimensional dendritic molecular architecture with high content of functional groups, low viscosity and high solubility.<sup>1</sup> HPs have been applied in some fields including coatings, processing additives and electrolytes in lithium ion batteries.<sup>2</sup> However, HPs have never been used as electrode materials probably due to the difficulty in the design of desired molecular structures.

On the other hand, Li-S battery is emerging as a new kind of lithium ion battery. Organosulfur compounds and sulfurized carbons are being explored to be used as cathode materials in lithium ion batteries, aimed at exceeding the performance of marketable products like LiCoO<sub>2</sub> and LiMnO<sub>2</sub>.<sup>3</sup> However, the energy density of such kind of Li-S batteries was hard to be improved since it was fairly difficult to obtain organosulfur compounds and sulfurized carbons with sulfur content over 50 wt %.<sup>4</sup> Additionally, sulfurized carbons usually need tedious thermal treatments above 250 °C, due to their poor solubility.<sup>5</sup> Recently, Pyun and co-workers addressed such a challenge *via* bulk inverse vulcanization, which was copolymerization of a large percentage of sulfur (50-99 wt %) and a modest amount of DIB (1-50 wt %). It exhibited high specific capacity and stability

when using these copolymers as cathode-active materials in Li-S battery.<sup>6</sup> However, gelation usually occurs in the bulk polymerization of such a “A<sub>2</sub> + B<sub>4</sub>” system, leading to hard processibility below the thermal decomposition temperature of these polymers. Therefore, polymers with high sulfur content and high solubility are eagerly expected.

Herein, we synthesized a kind of SIVHPs *via* RROP of S<sub>8</sub> with DIB in solution. These SIVHPs possess relatively high molecular weights and excellent solubility in organic solvents (up to 400 mg mL<sup>-1</sup>). When modified *via* sequential thiol-ene and Menschutkin click reactions, SIVHPs were endowed with water solubility for the first time. The solution of SIVHPs in CHCl<sub>3</sub> was absorbed into GUAs<sup>7</sup> and used as cathode-active materials in Li-S batteries. The Li-S batteries showed high coulombic efficiency (~100%), superior cycling performance and good rate capability.

### Experimental

#### Materials

DIB, 2,2-dimethoxy-2-phenyl-acetophenone (DMPA) were purchased from TCI Shanghai. 3-(Dimethylamino)-1-propanethiol was acquired from Atomax Chem Co. Ltd. Sublimed sulfur, chloroform (CHCl<sub>3</sub>), dimethylformamide (DMF), tetrahydrofuran (THF), toluene, 1,4-dioxane, anisole, N-methyl-2-pyrrolidone (NMP) and other organic solvents were purchased from Sinopharm Chemical Reagent Co. Ltd. DIB was

passed through a column of basic alumina before use and all the other materials were used as received.

### Instrumentation

Gel permeation chromatography (GPC) was recorded on a Perkin Elmer HP 1100, using THF as the eluent at a flow rate of 1 mL min<sup>-1</sup>, RI-WAT 150 CVt+ as the detector and linear polystyrene for calibration at 40 °C for characterization of apparent molecular weights. <sup>1</sup>H NMR (400 MHz) spectroscopy measurements were carried out on a Varian Mercury plus 400 NMR spectrometer. <sup>13</sup>C NMR (500 MHz) measurements were carried out on an Avance III 500 NMR spectrometer. Fourier transform infrared (FTIR) spectra were recorded on a PE Paragon 1000 spectrometer (film or KBr disk). UV-visible spectra were obtained by using a Varian Cary 300 Bio UV-visible spectrophotometer. Thermogravimetric analysis (TGA) was carried out on a Perkin-Elmer Pyris 6 TGA instrument under nitrogen with a heating rate of 10 °C min<sup>-1</sup>. SEM images were obtained by a Hitachi S4800 field-emission SEM system. The cells were discharged and charged on a LAND electrochemical station (Wuhan) from 1.0 to 3.0 V at a current density of 100 mA g<sup>-1</sup> sulfur to test the cycle life. Cyclic voltammograms (CV) were recorded on a CHI604c electrochemical workstation (Shanghai Chenhua) between 1.0 and 3.0 V to characterize the redox behavior and the kinetic reversibility of the cell.

### Synthesis of soluble inverse-vulcanized hyperbranched polymers with S<sub>8</sub> and DIB

S<sub>8</sub> and DIB were mixed in CHCl<sub>3</sub> with feed molar ratios of S<sub>8</sub> to DIB from 2 to 8. The reaction was taken in an autoclave under N<sub>2</sub> atmosphere followed by heating to 150 °C~180 °C for 0.5-7 hours. After cooling down to room temperature, the solution was precipitated with n-hexane. After being dried, the orange-red product was achieved (Yield: 35%-80%). <sup>1</sup>H NMR (400 MHz, CDCl<sub>3</sub>), δ (ppm): 7.32 (C<sub>6</sub>H<sub>4</sub>), 5.63-4.94 (C=CH<sub>2</sub>), 4.26-2.48 (S<sub>n</sub>-CH<sub>2</sub>-C), 2.37-0.44 (C-CH<sub>3</sub>). <sup>13</sup>C NMR (500 MHz, CDCl<sub>3</sub>), δ (ppm): 146.5-137.1, 129.9-120.5, 117.6, 112.8, 59.4-41.5, 33.7-11.6. FTIR: 2967.24 (C-H), 1598.24 (C=C), 1537.32-1340.99 (C-H), 1213.91 (C-C), 855.08-650.48 (C-H), 486.50 (C-S) cm<sup>-1</sup>.

### Synthesis of quaternary ammonium SIVHPs

SIVHPs (0.04 g, 1 mmol), 3-(dimethylamino)-1-propanethiol (DPT) (0.60 g, 5 mmol) and DMPA (21 mg, 0.08 mmol) were added into dried toluene (2 mL) in a 25 mL round-bottom flask. After being sealed, the mixture was bubbled with N<sub>2</sub> for 15 min to eliminate oxygen. Then, the reaction was triggered by UV-irradiation at 365 nm for 4 hours under stirring at room temperature. The solution was subsequently diluted with 8 mL dried DMF and cooled down to 0 °C. Another DMF (3 mL) solution of 3-bromo-1-propyne (14 mg, 1.2 mmol) was added into the DMF solution above dropwise under vigorous stirring. The mixture was further stirred overnight and added into diethyl ether solution dropwise for precipitation at 0 °C to afford orange precipitates. After being dried in vacuum at room temperature, quaternary ammonium SIVHPs were achieved. <sup>1</sup>H NMR (400 MHz, DMSO), δ (ppm): 7.94-7.24 (C<sub>6</sub>H<sub>4</sub>), 4.00-3.73 (2H, CH<sub>2</sub>-C≡CH), 3.60-3.39 (2H, C<sub>6</sub>H<sub>4</sub>-CH<sub>2</sub>-CH<sub>2</sub>-CH<sub>2</sub>-N<sup>+</sup>), 3.24-3.00 (7H, C≡CH, N<sup>+</sup>(CH<sub>3</sub>)<sub>2</sub>), 3.00-2.92 (2H, C<sub>6</sub>H<sub>4</sub>-CH-CH<sub>2</sub>-S), 2.85-2.73

(2H, S-CH<sub>2</sub>-CH<sub>2</sub>-CH<sub>2</sub>-N<sup>+</sup>), 2.25-1.96 (4H, C<sub>6</sub>H<sub>4</sub>-CH<sub>2</sub>-CH<sub>2</sub>-S, S-CH<sub>2</sub>-CH<sub>2</sub>-CH<sub>2</sub>-N<sup>+</sup>). <sup>13</sup>C NMR (500 MHz, DMSO), δ (ppm): 145.3-121.7, 82.8, 72.0, 61.7, 53.3, 49.8, 34.5, 33.7, 21.6-21.3.

### Preparation of GUAs via the "sol-cryo" method

Graphene oxide was prepared by chemical exfoliation of graphite according to the previous protocol.<sup>8</sup> Typically, the aqueous graphene oxide and CNTs with the same concentration of 6.0 mg mL<sup>-1</sup> were mixed and stirred with a magnetic bar for 1.5 h, and then poured into a mold followed by freeze-drying for 2 days. The as-prepared GO/CNTs foam with a known density of 6.0 mg mL<sup>-1</sup>. After being chemically reduced by hydrazine vapor at 90 °C for 24 h and then vacuum-dried at 90 °C for 24 h, GUAs were achieved.<sup>7</sup>

### Fabrication of Li-S batteries and electrochemical measurements

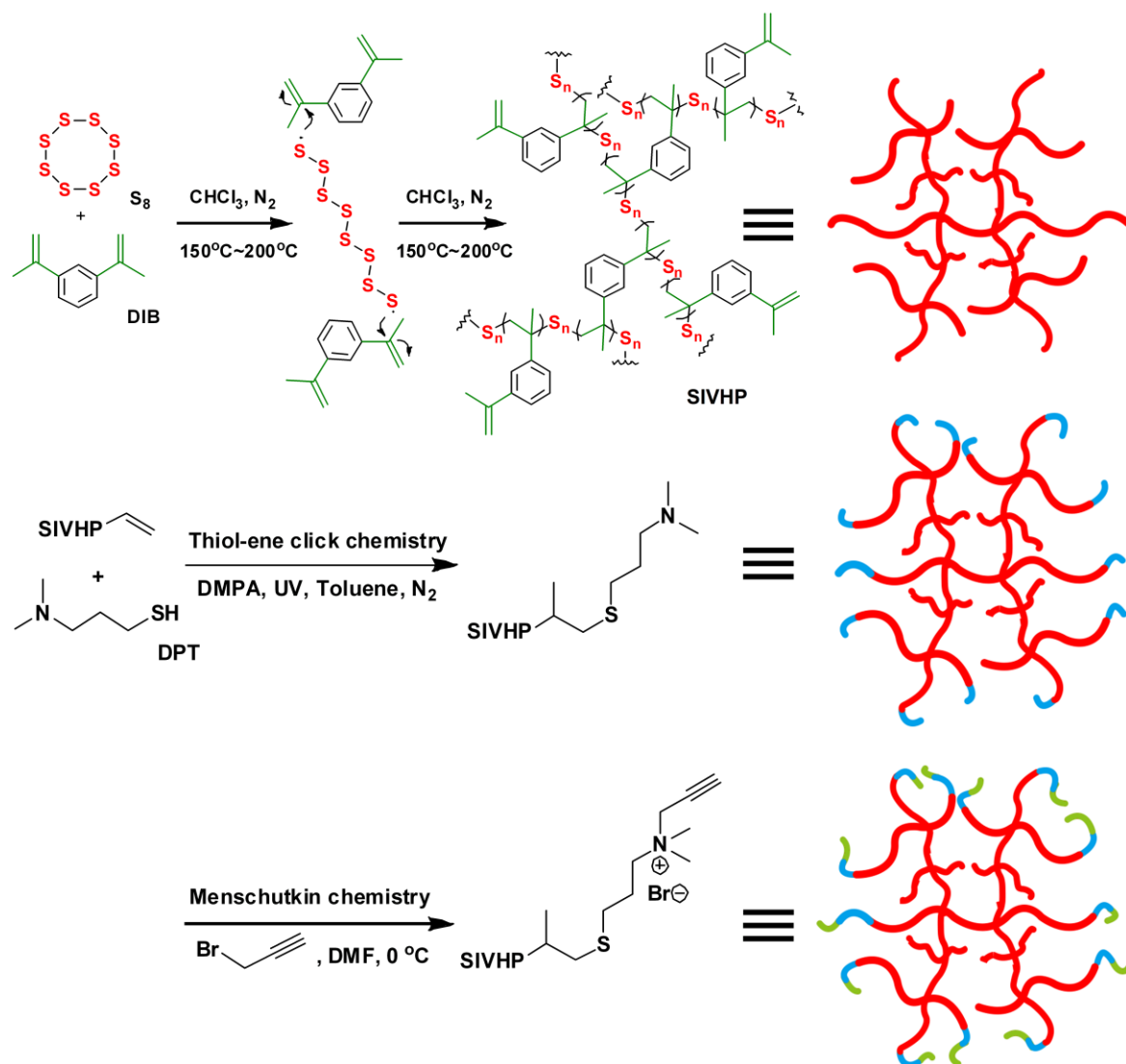
SIVHP (0.85 g) in CHCl<sub>3</sub> were added into GUAs (0.15 g) dropwise. The as-made materials were dried in a vacuum oven at 30 °C for 12 h to remove the solvent. The SIVHP-GUAs was mixed with poly (vinylidene fluoride) (PVDF 900), acetylene black (AB), and N-methyl-2-pyrrolidinone (NMP, anhydrous) to form a cathode slurry. The ratio of SIVHP-GUAs: AB: PVDF was 7.5: 1: 1.5 by weight. After mixing homogeneously overnight by magnetic stirring, the slurry was cast onto an aluminium current collector using a doctor blade. The control sulfur-GUAs cathode containing 60 wt % sulfur-GUAs, 20 wt % AB and 20 wt % PVDF binder was prepared in the same way. The coated electrodes were dried in a vacuum oven at 60 °C for 48 h. Subsequently, the electrode was cut into disks with a diameter of 11 mm. Coin-type (CR2025) cells were assembled in an argon-filled glove box to avoid contamination of moisture and oxygen. The electrolyte used in this work was 1 mol L<sup>-1</sup> LiTFSI in a solvent mixture of 1,3-dioxolane (DOL) and dimethoxymethane (DME) (1:1 v/v).

## Results and discussion

### Synthesis and characterization of SIVHPs via RROP of S<sub>8</sub> and DIB in solution

In the RROP to synthesize SIVHPs, S<sub>8</sub> and DIB were chosen as A<sub>2</sub> and B<sub>4</sub> monomers. The diradical moiety from thermal fracture of S<sub>8</sub> could react with C=C bonds of DIB via efficient RROP, as shown in Scheme 1.<sup>9</sup> S-S bonds were subjected to reversible rupture and formation during the reaction processes. Along with the increasing of viscosity during polymerization, the movements of free radicals were obstructed, and the main trend of chain growth was gradually replaced by chain rupture.<sup>10</sup> We can infer that low viscosity together with relatively strong free radical activity afforded large molecular weights and high degree of branching. This was why polymerization in solution environment was preferred over bulk polymerization. Meanwhile, the branching molecular architecture without gelation should endow HPs with better solubility than copolymers by bulk polymerization.

After the polymerization, SIVHPs with relatively high molecular weight were obtained. Polymerization data were gains



**Scheme 1** Synthesis of SIVHPs *via* RROP and subsequent functionalization by thiol-ene and Menshutkin click chemistry.

5 *via* GPC (see Table 1), and feed molar ratio-, reaction time-, and temperature-dependent GPC curves were presented in Fig. 1, showing the influence of reaction parameters. The polymerization in solution afforded the SIVHPs with the largest  $M_n$  of 5400 g mol<sup>-1</sup> and  $M_w$  of 2 3500 g mol<sup>-1</sup> when the reaction parameters  
 10 were set as 180 °C, 0.5 hour, and 4 as the feed molar ratio of S<sub>8</sub> to DIB. In comparison, the highest  $M_n$  achieved by bulk polymerization was only 1260 g mol<sup>-1</sup>.<sup>6</sup> When the temperature and reaction time increased, molecular weight increased at the beginning and then decreased (Fig. 1a, 1b, 1d and 1e) likely due  
 15 to the rupture of S-S bonds. We also found that the polydispersity index (PDI) increased together with the molecular weight (Table 1), which indirectly proved the hyperbranched polymerization of SIVHPs.<sup>11</sup> All above demonstrated the obvious advantage of solution polymerization over bulk polymerization in the synthesis  
 20 of SIVHPs.

The structure of the resulting SIVHPs was characterized *via* <sup>1</sup>H NMR and <sup>13</sup>C NMR spectroscopy shown in Fig. 2a and 2b. In the

<sup>1</sup>H NMR spectrum (Fig. 2a), the proton signal of the methylene group (labelled as “a”) was observed at 2.48-4.26 ppm, which  
 25 was influenced by lengths of the linear polysulfane chains linked up with methylene group. It indicated that C-S bonds were successfully formed.<sup>12</sup> In the <sup>13</sup>C NMR spectrum (Fig. 2b), the methylene carbon signal (labelled as “a and c”) which was located at 41.54-59.42 ppm implied the existence of C-S bonds.  
 30 Notably, the signal split into two at around 44.25 ppm and 54.65 ppm, maybe due to the electron withdrawing effect of linear polysulfane with different lengths. FTIR spectra of monomer and SIVHP are also presented in Fig. S1†, in which the signal at 486.50 cm<sup>-1</sup> belonged to C-S bonds.<sup>13</sup> In addition, UV-vis spectra of DIB and SIVHPs are shown in Fig. 3a for comparison.  
 35 Compared with the pure DIB peak at 246 nm, the wider peak at 240 nm resulted from the reduced conjugated structure originated from the polymerization process. Notably, a blue-shifted wide shoulder peak at around 290 nm was observed, which could be  
 40 assigned to the R-S<sub>n</sub>-R groups.<sup>14</sup> SIVHP -1 and SIVHP -2

**Table 1.** Reaction conditions and selected results for the synthesis of SIVHPs via RROP of S<sub>8</sub> and DIB in CHCl<sub>3</sub>.

Entry	$\gamma$ <sup>a</sup>	Temperature/°C	Time/h	$M_n^b$ (g mol <sup>-1</sup> )	$M_w^b$ (g mol <sup>-1</sup> )	$M_p^b$ (g mol <sup>-1</sup> )	PDI <sup>b</sup>
1	4:1	150	0.5	1300	2100	1200	1.62
2	4:1	160	0.5	1400	2400	1200	1.71
3	4:1	170	0.5	1500	2400	1400	1.60
4	4:1	180	0.5	5400	23500	6200	4.35
5	4:1	190	0.5	2900	5100	2800	1.76
6	4:1	200	0.5	2600	6300	3000	2.42
7	4:1	180	0.25	1600	6500	1900	4.06
8	4:1	180	0.75	4200	18200	5000	4.33
9	4:1	180	1	2800	7000	2800	2.50
10	4:1	180	2	2200	6200	2700	2.82
11	4:1	180	3	1900	3900	2400	2.05
12	4:1	180	5	1300	2500	1800	1.92
13	4:1	180	7	1100	2200	1600	2.00
14	8:1	180	0.5	2600	5300	2400	2.04
15	8:3	180	0.5	3000	5800	3100	1.93
16	8:4	180	0.5	2900	4300	3000	1.48
17	8:5	180	0.5	2700	3600	2900	1.33

<sup>a</sup> Feed molar ratios ( $\gamma$ ) of S<sub>8</sub> to DIB. <sup>b</sup> Number-averaged molecular weight ( $M_n$ ), weight-averaged molecular weight ( $M_w$ ), peak value of  $M_n$  ( $M_p$ ) and polydispersity index (PDI) determined by GPC.

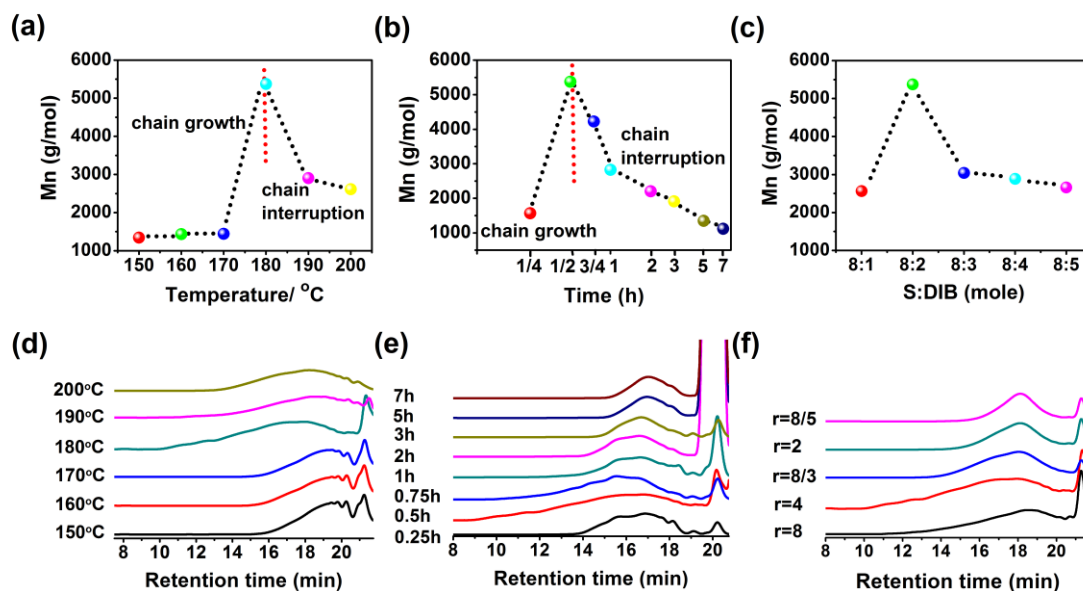


**Fig. 1.** Dependence of  $M_n$  on (a) temperature (150–200 °C), (b) time (0.25–7 h) and (c) feed molar ratios ( $\gamma = 8/5, 2, 8/3, 4, 8$ ) of S<sub>8</sub> to DIB. GPC peak evolution depending on (d) temperature (150–200 °C), (e) time (0.25–7 h) and (f) feed molar ratios ( $\gamma = 8/5, 2, 8/3, 4, 8$ ) of S<sub>8</sub> to DIB.

possess different feed molar ratios of S<sub>8</sub> to DIB with 8 and 2, respectively. UV-vis spectra of them showed different intensities because of their different amount of R-S<sub>n</sub>-R groups.

We further investigated thermal properties of SIVHPs. Curves of differential scanning calorimetry (DSC) are shown in Fig. 3b with different feed molar ratios ( $\gamma$ ) of S<sub>8</sub> to DIB with 8, 4, 8/3 and 2. The corresponding glass transition temperatures ( $T_g$ ) were 24.1 °C, 16.3 °C, 4.4 °C, and -0.5 °C, respectively. The  $T_g$  data of SIVHPs revealed that higher content of the utilized DIB led to lower  $T_g$ . When a higher feed molar ratio ( $\gamma$ ) of S<sub>8</sub> to DIB was used, both of the C=C bonds in DIB would probably participate

in the polymerization, introducing more rigid benzene rings into the molecular chain, thus higher  $T_g$  was obtained. On the contrary, smaller feed molar ratio led to less benzene rings in the molecular chains and lower  $T_g$ . TGA curves show that SIVHPs and neat sulfur started to decompose at 170 °C (Fig. S2†), which made them difficult to be melting processed.

In general, we observed that SIVHPs were orange-red intrinsically (Fig. 4b), which were originated from yellow-coloured sulfur (Fig. 4a). SIVHPs were dissolved in CHCl<sub>3</sub> (Fig. 4c) with the utmost concentration of 400 mg mL<sup>-1</sup> at room temperature, and did not undergo any precipitation after settling

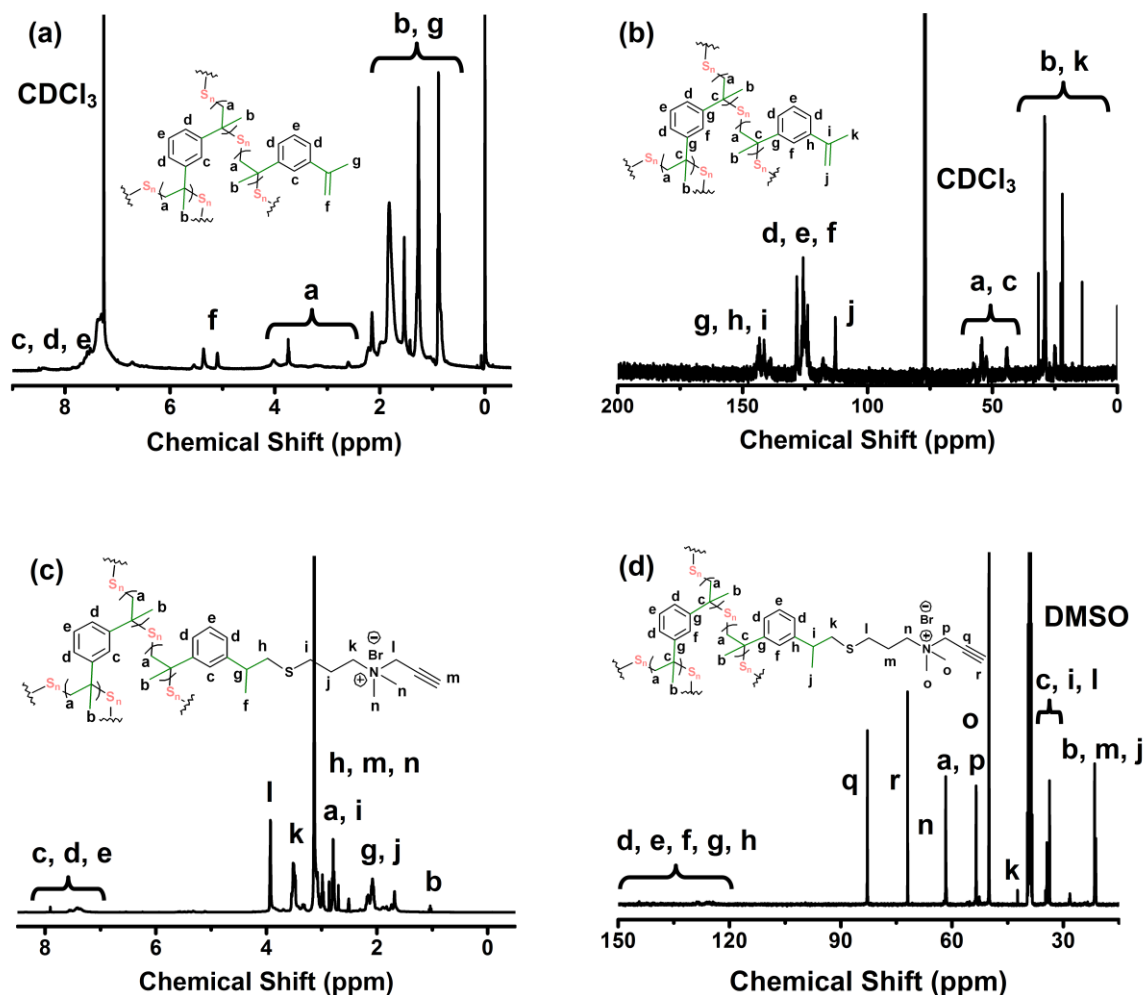


**Fig. 2** (a)  $^1\text{H}$  NMR spectrum of SIVHP in  $\text{CDCl}_3$ . (b)  $^{13}\text{C}$  NMR spectrum of SIVHP in  $\text{CDCl}_3$ . (c)  $^1\text{H}$  NMR spectrum of quaternary ammonium SIVHP in DMSO. (d)  $^{13}\text{C}$  NMR spectrum of quaternary ammonium SIVHP in DMSO.

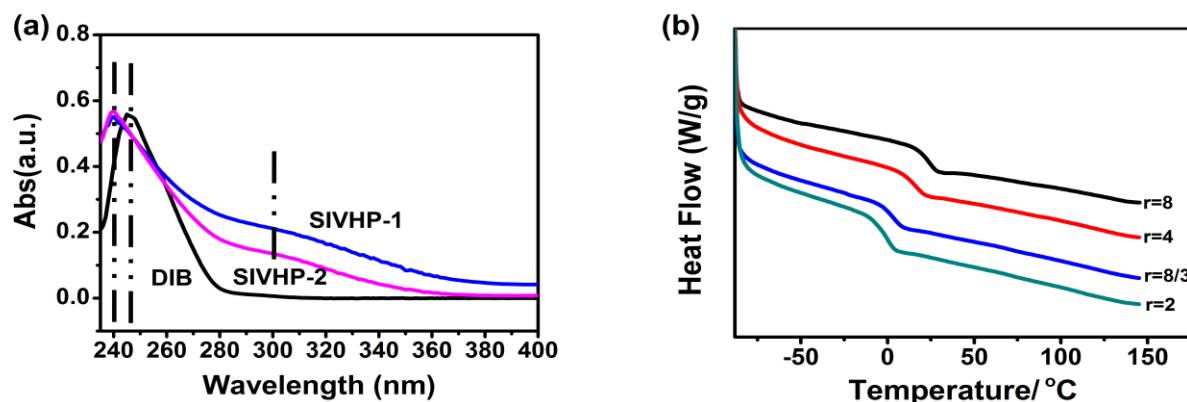


**Fig. 3** (a) UV-Vis spectra of DIB and SIVHP-1 (feed molar ratio of  $\text{S}_8$  to DIB was 8) and SIVHP-2 (feed molar ratio of  $\text{S}_8$  to DIB was 2). (b) DSC of SIVHPs with feed molar ratios ( $r = 8/5, 2, 8/3, 4, 8$ ) of  $\text{S}_8$  to DIB from 2 to 8, indicating the  $T_g$  of 24.1  $^\circ\text{C}$ , 16.3  $^\circ\text{C}$ , 4.4  $^\circ\text{C}$ , -0.5  $^\circ\text{C}$ , respectively.

for one month, superior to the limited solubility of bulk copolymers. As shown in Fig. 4h and 4i, 15 mg SIVHP could be dissolved in 2 mL  $\text{CHCl}_3$  within 5 minutes, while bulk copolymers of  $\text{S}_8$  and DIB presented weaker and slower solubility

with the same sulfur content of 70 wt % in polymers. The described SIVHPs presented good solubility in various organic solvents, such as toluene,  $\text{CHCl}_3$ , DMF, 1,4-dioxane, THF and anisole (Fig. 4j). In Fig. 4e, SIVHPs were spin-coated on the

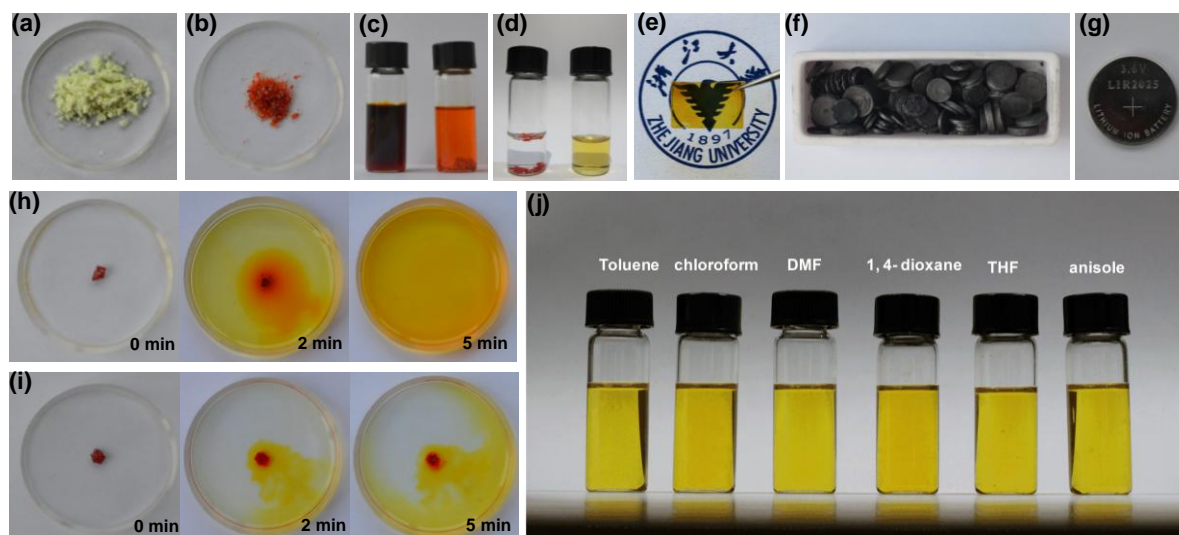


**Fig. 4** Digital photographs of (a) sulfur, (b) SIVHP, (c) 800 mg SIVHP (left) and bulk polymer of S and DIB (right) with 70 wt % sulfur content immersed in 2 mL chloroform at room temperature, (d) SIVHP (left) and quaternary ammonium SIVHP (right) immersed in water at room temperature, (e) film spin-coated with SIVHP solution on PET, (f) diverse-sized GUAs, (g) a Li-S battery we fabricated. Dissolution process of (h) SIVHP and (i) bulk polymer with the same feed molar ratios ( $\gamma$ ) of  $S_8$  to DIB within 5 min. (j) SIVHP dissolved in toluene, chloroform, DMF, 1,4-dioxane, THF and anisole.

transparent substrate to form transparent films, which further elucidated their fine solution processibility.

#### Synthesis and characterization of quaternary ammonium SIVHPs

SIVHPs presented excellent solubility in organic solvents but not in water. In order to expand their applications, the functionalized quaternary ammonium SIVHPs were synthesized *via* thiol-ene and Menshutkin reactions. SIVHPs were modified with sulfhydryl through thiol-ene click chemistry of thiols and C=C bonds under UV initiation, followed by Menshutkin click reaction with propargyl bromide. The reaction mechanism is shown in Scheme 1.<sup>15</sup>

Different from SIVHPs, the quaternary ammonium SIVHPs showed superior solubility in water, which directly demonstrated the chemical conversion from SIVHPs to quaternary ammonium SIVHPs (Fig. 4d). The structure of quaternary ammonium SIVHPs were characterized *via*  $^1\text{H}$  NMR and  $^{13}\text{C}$  NMR spectroscopy shown in Fig. 2c and 2d. In the  $^1\text{H}$  NMR spectrum (Fig. 2c), the disappearance of vinyl protons and the proton signal of alkynyl protons proved that functionalization was successfully completed. In the  $^{13}\text{C}$  NMR spectrum (Fig. 2d), the alkynyl carbon signal labelled as "r" located at 71.97 ppm also implied the successful modification. In short, SIVHPs had the capacity to be modified, and offered a larger range of solution processibility and new opportunities to fabricate water-soluble, amphiphilic sulfur-rich species.

#### Electrochemical measurements

Li-S battery is receiving interest for their outstanding merits such as the ultrahigh theoretical energy capacity of  $1672\text{ mA h g}^{-1}$ , the high theoretical specific energy of  $2600\text{ W h kg}^{-1}$  and environmentally friendly operation.<sup>16</sup> However, intermediate lithium polysulfides, which generated from stepwise reduction

reactions during the discharge processes, would dissolve in the liquid electrolytes and shuttle between the anode and cathode.<sup>17</sup> The shuttle effect, along with the raised resistance of sulfur, intensively degraded the stability and increased pointless cost of sulfur-active materials.<sup>18</sup> Due to all these problems, a big gap existed between practical performance and theoretical expectation upon cycle life, specific capacity and energy efficiency of Li-S batteries.<sup>19</sup>

In view of the excellent solution processibility of the SIVHPs, they were assembled into conductive frameworks of GUAs by facile fluid infiltration, playing the role of cathode-active materials in Li-S batteries. The GUAs previously reported by our group were constructed with cell walls of giant graphene sheets and CNTs ribs, which possessed superior electroconductivity, large surface area ( $\sim 272\text{ m}^2\text{ g}^{-1}$ ), and super-high absorption capacities for organic solvents.<sup>7</sup> In order to achieve strong skeleton and dense holes, we fabricated GUAs with a density of  $6.0\text{ mg mL}^{-1}$  (Fig. 4f). Element mapping images and energy-dispersive X-ray (EDX) analysis further illuminated the homogeneous and abundant distribution of sulfur element in GUAs (Fig. 5), indicating effective infiltration of SIVHPs along the walls of aerogels. Efficient connected network would improve the electrical conductivity of cathode materials, and thus improve the charge-discharge efficiency.<sup>20</sup>

Coin cells (2025, Fig. 4g) consisting of Li-foil anodes and SIVHPs-GUAs composite cathodes were tested to examine the electrochemical performance. An initial specific discharge capacity of  $1247.6\text{ mA h g}^{-1}$  with long-term cycle stability of  $694.0\text{ mA h g}^{-1}$  after 90 cycles are shown in Fig. 6c at a rate of  $0.1\text{C}$  ( $1\text{C} = 1672\text{ mA g}^{-1}$ ), which outdistanced the performance of pure sulfur ( $449.9\text{ mA h g}^{-1}$  after 90 cycles). The content of sulfur in SIVHPs was determined to be  $\sim 75\text{ wt \%}$  by TGA (Fig. 5f).

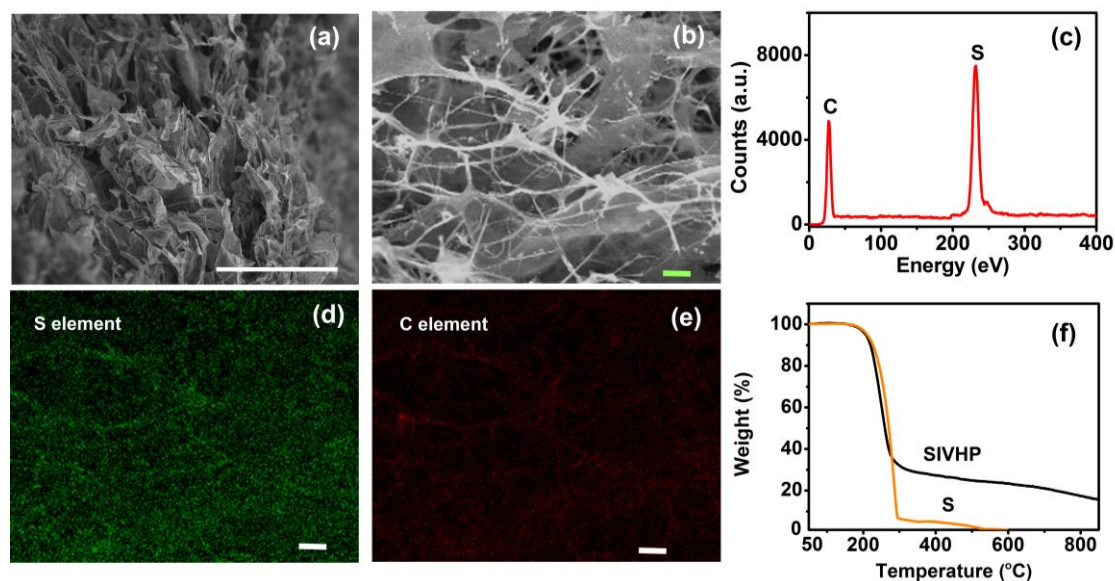


**Fig. 5** (a) SEM image of GUA ( $\rho = 6 \text{ mg mL}^{-3}$ ), (b) SEM image of SIVHPs-GUAs composite. (c) EDX spectrum of SIVHPs-GUAs composite. (d) Elemental mapping of sulfur. (e) Elemental mapping of carbon. (f) TGA curves measured for sulfur and SIVHP. Scale bars are  $50 \mu\text{m}$  (a) and  $10 \mu\text{m}$  (b, d, e).

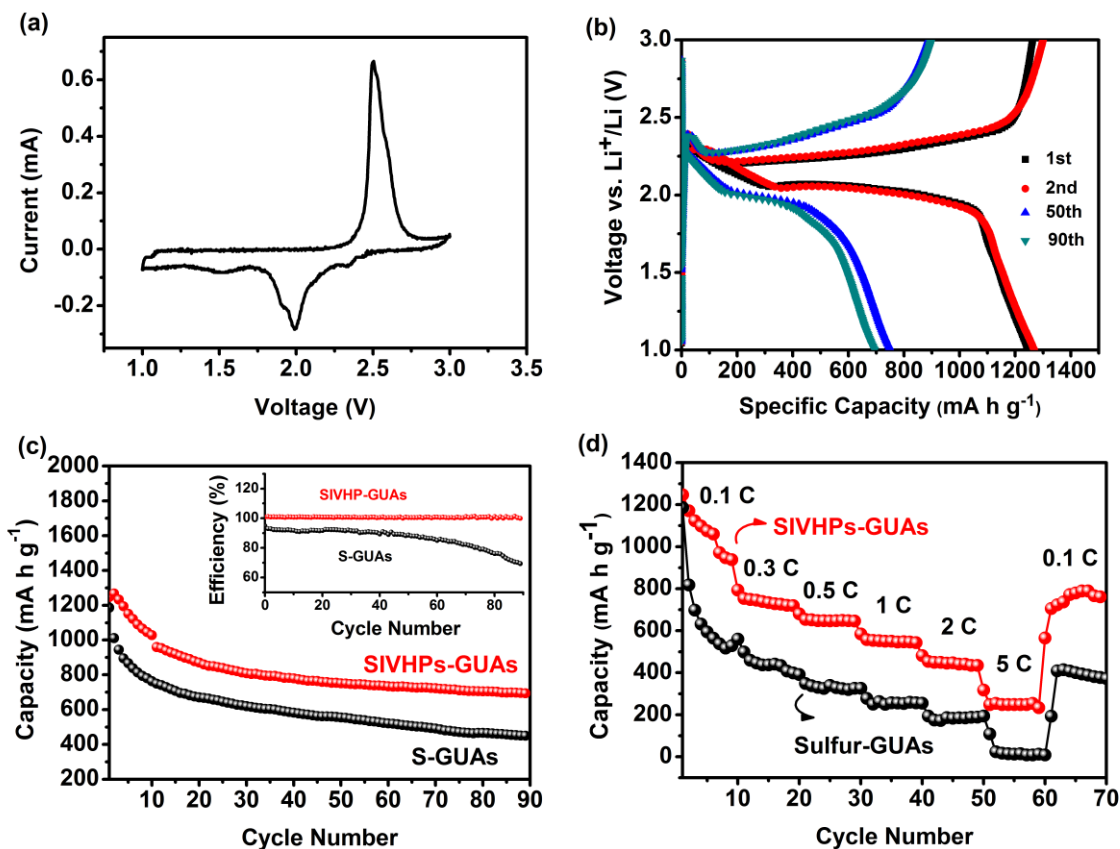


**Fig. 6** Electrochemical measurements of SIVHPs-GUAs as Li-S battery cathode materials. (a) Cyclic voltammetry of SIVHPs-GUAs at  $0.1 \text{ mV s}^{-1}$  in a potential window from 1.0 to 3.0 V vs  $\text{Li}^+/\text{Li}$ . (b) Charge/discharge profiles of the SIVHPs-GUAs cathode at a current rate of 0.2C. (c) Coulombic efficiency of sulfur and SIVHPs-GUAs at 0.1 C for 90 cycles, and inset for galvanic charge-discharge performance of SIVHPs-GUAs at 0.1 C for 90 cycles. (d) Rate capabilities of SIVHPs-GUAs and S-GUAs composite cathodes.

In order to explore the mechanism, CV of the cells were tested with a scan rate of  $0.1 \text{ mV s}^{-1}$  between 1.0 and 3.0 V versus



Li/Li<sup>+</sup>, which were made with SIVHPs-GUAs as the cathode-active materials (Fig. 6a). The reduction peaks at potentials of 2.3 V and 2.0 V were respectively corresponded to the formation of long-chain Li<sub>2</sub>S<sub>n</sub> (4 ≤ n ≤ 8) and lower-order Li<sub>2</sub>S<sub>n</sub> (2 ≤ n ≤ 4).  
 5 The broad reduction current peak at ~1.5 V suggested a solid-to-solid phase transition (from SIVHP to Li<sub>2</sub>S). In the anodic scan, only one oxidation peak at 2.5 V was observed, which was related to the conversion of Li<sub>2</sub>S and/or short-chain polysulfides to long-chain polysulfides.<sup>21</sup> Fig. 6b showed the galvanostatic charge/discharge curves in the 1st, 2nd, 50th, and 90th cycles at a current rate of 0.1C. Corresponding to the CV profiles, two plateaus were assigned to the formation of long-chain polysulfides (high plateau at 2.3 V) and lower-order Li<sub>2</sub>S<sub>n</sub> (low plateau at 2.0 V) during the discharge process.

15 Notably, the coulombic efficiency of SIVHPs-GUAs at 0.1 C was all around 100% during 90 cycles (Fig. 6c, inset). In contrast, sulfur-GUAs exhibited decreasing coulombic efficiency from 94.8 to 69.6%, which was caused by a serious shuttle effect due to the lack of chemical fixation of neat sulfur.<sup>22</sup> Galvanic current  
 20 measurements were taken to evaluate the rate performance of the SIVHPs-GUAs and sulfur-GUAs composite electrode (Fig. 6d). SIVHPs-GUAs showed capacities of 1217, 796, 685, 583, 482, and 255 mA h g<sup>-1</sup> at the current rates of 0.1, 0.3, 0.5, 1, 2 and 5C after 10 cycles, respectively. In addition, after the rate test for 60  
 25 cycles, a reversible discharge capacity of 800 mA h g<sup>-1</sup> was maintained when it returned to 0.1 C. By contrast, neat sulfur-GUAs exhibited a rapid and massive loss of capacities (1192, 506, 348, 284, 196 and 27 mA h g<sup>-1</sup> at the current rates of 0.1, 0.3, 0.5, 1, 2 and 5C respectively after 10 cycles). We proposed that the  
 30 good performance of the SIVHPs-GUAs composite electrode was attributed to the chemical fixation of sulfur *via* hyperbranched polymerization.

## Conclusions

In this work, we prepared soluble inverse-vulcanized  
 35 hyperbranched polymers *via* facile RROP of S<sub>8</sub> and DIB in solution. Modification *via* thiol-ene and Menshutkin reactions endowed the sulfur-rich polymers with water-solubility. The hyperbranched polymers were proved to be solution processible and possessed good electrochemical performance exceeding neat  
 40 sulfur. In view of the attributes of large surface area and electroconductibility, we introduced graphene-CNTs aerogels to support the hyperbranched polymers as new cathode-active materials in Li-S batteries. Due to their high solubility, excellent solution processibility, clickable multifunctional groups, and  
 45 superior electrochemical performance, the sulfur-rich hyperbranched polymers are promising in many applications such as Li-S batteries, host-guest encapsulation, and drugs.

## Acknowledgements

This work is supported by the National Natural Science  
 50 Foundation of China (No. 51173162 and No. 21325417), Fundamental Research Funds for the Central Universities (No. 2013XZZX003), and China Postdoctoral Science Foundation (2014M551724).

## Notes and references

- 55 <sup>a</sup> MOE Key Laboratory of Macromolecular Synthesis and Functionalization, Department of Polymer Science and Engineering, Zhejiang University, 38 Zheda Road, Hangzhou, P. R. China. E-mail: chaogao@zju.edu.cn  
<sup>b</sup> State Key Laboratory of Silicon Materials, Key Laboratory of Advanced  
 60 Materials and Applications for Batteries of Zhejiang Province & Department of Materials Science and Engineering, Zhejiang University, Hangzhou 310027, P.R. China. Tel./fax: +86 0571 87952615; E-mail: gaomx@zju.edu.cn (M. Gao).  
<sup>c</sup> College of Chemistry and Chemical Engineering, Yantai University, 30  
 65 Qingquan Road, Yantai 264005, P. R. China.  
 † Electronic Supplementary Information (ESI) available: Differential scanning calorimetry for preparation of SIVHPs, FTIR spectra and TGA curves for SIVHPs. See DOI: 10.1039/b000000x/.
- 1 P. Flory, *J. Am. Chem. Soc.*, 1952, **74**, 2718; C. Gao and D. Y. Yan, *Prog. Polym. Sci.*, 2004, **29**, 183; D. Yan, C. Gao and H. Frey, *Hyperbranched Polymers: Synthesis, Properties and Applications*, John Wiley & Sons, Hoboken, NJ, 2011; B. Voit, *J. Polym. Sci. Part A: Polym. Chem.*, 2000, **38**, 2505; M. Jikei, M. Kakimoto, *Prog. Polym. Sci.*, 2001, **26**, 1233; C. Gao, S. Muthukrishnan, W. Li, J. Yuan, Y. Xu and A. H. E. Müller, *Macromolecules*, 2007, **40**, 1803.
  - 2 C. C. Lee, J. A. MacKay, J. M. J. Frechet, F. C. Szoka, *Nat. Biotechnol.*, 2005, **23**, 1517; Y. K. Jeong, T. W. Kwon, I. Lee, T. S. Kim, A. Coskun and J. W. Choi, *Nano Lett.*, 2014, **14**, 864; Y. Liang, Z. Tao and J. Chen, *Adv. Energy Mater.*, 2012, **2**, 742; D. M. Tigelaar, M. A. B. Meador, J. D. Kinder and W. R. Bennett, *Macromolecules*, 2006, **39**, 120; T. Itoh, Y. Ichikawa, T. Uno, M. Kubo and O. Yamamoto, *Solid State Ionics*, 2003, **156**, 393.
  - 3 J. M. Tarascon and M. Armand, *Nature*, 2001, **414**, 359; A. S. Aricò, P. Bruce, B. Scrosati, J. M. Tarascon, W. V. Schalkwijk, *Nat. Mater.* 2005, **4**, 366; P. G. Bruce, B. Scrosati, J. M. Tarascon, *Angew. Chem. Int. Ed.*, 2008, **47**, 2930; M. S. Whittingham, *Chem. Rev.*, 2004, **104**, 4271; S. S. Zhang, *Frontiers in Energy Research*, 2013, **1**, 10.
  - 4 K. Naoi, K. I. Kawase, M. Mori and M. Komiyama, *J. Electrochem. Soc.*, 1997, **144**, L173; F. Wu, S. X. Wu, R. J. Chen, J. Z. Chen and S. Chen, *Electrochem. Solid State Lett.*, 2010, **13**, A29; S. Zhang, *Energy Storage*, 2013, **1**, 10.
  - 5 J. Wang, J. Yang, C. Wan, K. De, J. Xie and N. Xu, *Adv. Funct. Mater.*, 2003, **13**, 487; L. Xiao, Y. Cao, J. Xiao, B. Schwenzer, M. H. Engelhard, L. V. Saraf, Z. Nie, G. J. Exarhos and J. Liu, *Adv. Mater.*, 2012, **24**, 1176; Y. NuLi, Z. Guo, H. Liu and J. Yang, *Electrochem. Commun.*, 2007, **9**, 1913.
  - 6 W. J. Chung, J. J. Griebel, E. T. Kim, H. Yoon, A. G. Simmonds, H. J. Ji, P. T. Dirlamk, R. S. Glass, J. J. Wie, N. A. Nguyen, B. W. Guralnick, J. Park, Á. Somogyi, P. Theato, M. E. Mackay, Y. E. Sung, K. Char, J. Pyun, *Nat. Chem.*, 2013, **5**, 518; J. J. Griebel, S. Namnabat, E. T. Kim, R. Himmelhuber, D. H. Moronta, W. J. Chung, A. G. Simmonds, K. Kim, J. Laan, N. A. Nguyen, E. L. Dereniak, M. E. Mackay, K. Char, R. S. Glass, R. A. Norwood and L. J. Pyun, *Advanced Materials*, 2014, **26**, 3014; A. G. Simmonds, J. J. Griebel, J. Park, K. R. Kim, W. J. Chung, V. P. Oleshko, J. Kim, E. T. Kim, R. S. Glass, C. L. Soles, Y. Sung, K. Char and J. Pyun, *ACS Macro Lett.*, 2014, **3**, 229.
  - 7 H. Sun, Z. Xu, C. Gao, *Adv. Mater.* 2013, **25**, 2554; Z. Xu, C. Gao, *Acc. Chem. Res.*, 2014, **47**, 1267.
  - 8 Z. Xu, H. Sun, C. Gao, *APL Mater.*, 2013, **1**, 030901; T. Huang, B. Zheng, L. Kou, K. Gopalsamy, Z. Xu, C. Gao, Y. Meng, Z. Wei, *RSC Adv.*, 2013, **3**, 23957; Z. Xu, H. Sun, X. Zhao, C. Gao, *Adv. Mater.*, 2013, **25**, 188; Z. Xu, Y. Zhang, P. Li, C. Gao, *ACS Nano*, 2012, **6**, 7103; Z. Xu, C. Gao, *ACS Nano*, 2011, **5**, 2908; L. Kou, T. Huang, B. Zheng, Y. Han, X. Zhao, K. Gopalsamy, C. Gao, *Nat. Commun.*, 2014, **5**, 3754.
  - 9 C. Gao, S. Muthukrishnan, W. Li, J. Yuan, Y. Xu and A. H. E. Müller, *Macromolecules*, 2007, **40**, 1803; C. Gao, D. Yan and W. Chen, *Macromol. Rapid Commun.*, 2002, **23**, 465; Y. Han, C. Gao and X. He, *Sci. China: Chem.*, 2012, **55**, 604; S. P. Li, C. Gao, *Polym. Chem.*, 2013, **4**, 4450; J. Han, S. Li and C. Gao, *Macromolecules*, 2012, **45**, 4966.
  - 10 E. J. Goethals, *J. Macromol. Sci. Part C*, 1968, **2**, 1; H. W. Nesbitt, G. M. Bancroft, A. R. Pratt and M. J. Scaini, *Am. Min.*, 1998, **83**, 1067; R. Bellissent, L. Descotes, and P. Pfeuty, *J. Phys.: Condens. Matter*,

- 1994, **6**, A211; J. S. Tse and D. D. Klug, *Phys. Rev. B*, 1999, **59**, 34; R. Steudel, *Chem. Rev.*, 2002, **102**, 3905; L. B. Blight, B. R. Currell, B. J. Nash, R. T. M. Scott and C. Stillo, *Br. Polym. J.*, 1980, **12**, 5.
- 11 A. M. Fischer and H. Frey, *Macromolecules*, 2010, **43**, 8539; N. Clarke, E. D. Luca, J. M. Dodds, S. M. Kimani and L. R. Hutchings, *Eur. Polym. J.*, 2008, **44**, 665; X. Zhou, J. Zhu, M. Xing, Z. Zhang, Z. Cheng, N. Zhou and X. Zhu, *Eur. Polym. J.*, 2011, **47**, 1912.
- 12 E. J. Goethals, *Topics in Sulfur Chemistry*, Georg Thieme Verlag, Stuttgart, 1977; S. P. Li, J. Han and C. Gao, *Polym. Chem.*, 2013, **4**, 1774; H. Sun and C. Gao, *Biomacromolecules*, 2010, **11**, 3609; J. Han, B. Zhao, Y. Gao, A. Tang and C. Gao, *Polym. Chem.*, 2011, **2**, 2175.
- 13 E. Prestsch, P. Bühlmann, C. Affolter, *Structure Determination of Organic Compounds: Table of Spectra Data (third ed.)* Springer-Verlag, Berlin Heidelberg New York, 2000; I. Garcia-Lodeiro, A. Fernandez-Jimenez, M. T. Blanco-Varela, A. Palomo, *J. Sol-Gel Sci. Technol.*, 2008, **45**, 63.
- 14 C. Barchasz, F. Molton, C. Duboc, J.C. Leprêtre and S. Patoux, *Anal. Chem.*, 2012, **84**, 3973; Y. Li, H. Zhan, S. Liu, K. Huang, Y. Zhou, *J. Power Sources*, 2010, **195**, 2945; M. U. M. Patel, R. Demir-Cakan, M. Morcrette, J. M. Tarascon, M. Gaberscek, R. Dominko, *ChemSusChem*, 2013, **6**, 1177; L. Wang, X. He, J. Li, Gao, J. Guo, C. Jiang and C. Wan, *J. Mater. Chem.*, 2012, **22**, 22077; J. Rong, M. Ge, X. Fang, and C. Zhou, *Nano lett.*, 2014, **14**, 473.
- 25 15 J. Han, Y. Zheng, S. Zheng, S. Li, T. Hu, A. Tang and C. Gao, *Chem. Commun.*, 2014, **50**, 8712.
- 16 A. Manthiram, Y. Fu and Y. S. Su, *Acc. Chem. Res.*, 2012, **46**, 1125; S. Xin, Y. G. Guo and L. J. Wan, *Acc. Chem. Res.*, 2012, **45**, 1759; B. Scrosati and J. Garche, *J. Power Sources*, 2010, **195**, 2419; P. G. Bruce, S. A. Freunberger, L. J. Hardwick and J.M. Tarascon, *Nat. Mater.*, 2012, **11**, 19; S. S. Zhang and J. A. Read, *J. Power Sources*, 2012, **200**, 77; C. Liang, N. J. Dudney, J. Y. Howe, *Chem. Mater.*, 2009, **21**, 4724.
- 17 R. Chen, T. Zhao, J. Lu, F. Wu, L. Li, J. Chen, G. Tan, Y. Ye and K. Amine, *Nano lett.*, 2013, **13**, 4642; N. S. Choi, Z. Chen, S. A. Freunberger, X. Ji, Y. K. Sun, K. Amine, G. Yushin, L. F. Nazar, J. Cho and P. G. Bruce, *Angew. Chem. Int. Ed.*, 2012, **51**, 9994; Y. X. Yin, S. Xin, Y. G. Guo and L.J. Wan, *Angew. Chem. Int. Ed.*, 2013, **52**, 13186.
- 40 18 S. Evers and L. F. Nazar, *Acc. Chem. Res.*, 2012, **46**, 1135; G. Zhou, S. Pei, L. Li, D. Wang, S. Wang, K. Huang, L. Yin, F. Li and H. Cheng, *Adv. Mater.*, 2014, **26**, 625; L. Ji, M. Rao, H. Zheng, L. Zhang, Y. Li, W. Duan, J. Guo, E. J. Cairns and Y. Zhang, *J. Am. Chem. Soc.*, 2011, **133**, 18522; S. S. Zhang, *J. Power Sources*, 2013, **231**, 153; S. Evers, L.F. Nazar, *Acc. Chem. Res.*, 2013, **46**, 1135.
- 45 19 H. Wang, Y. Yang, Y. Liang, J. T. Robinson, Y. Li, A. Jackson, Y. Cui and H. Dai, *Nano lett.*, 2011, **11**, 2644; A. G. Simmonds, J. J. Griebel, J. Park, K. R. Kim, W. J. Chung, V. P. Oleshko, J. Kim, E. T. Kim, R. S. Glass, C. L. Soles, Y. E. Sung, K. Char and J. Pyun, *ACS Macro Lett.*, 2014, **3**, 229.
- 50 20 Y. Yang, G. Zheng, Y. Cui, *Chem. Soc. Rev.*, 2013, **42**, 3018; Y. Yang, G. Zheng, Y. Cui, *Chem. Soc. Rev.*, 2013, **42**, 3018; X. Ji, K. T. Lee and L. F. Nazar, *Nat. Mater.*, 2009, **8**, 500; N. Li, M. Zheng, H. Lu, Z. Hu, C. Shen, X. Chang, G. Ji, J. Cao and Y. Shi, *Chem. Commun.*, 2012, **48**, 4106; B. Zhang, X. Qin, G. Li, X. Gao, *Energy Environ. Sci.*, 2010, **3**, 153.
- 55 21 F. Wu, J. Chen, R. Chen, S. Wu, L. Li, S. Chen and T. Zhao, *The J. Phys. Chem. C*, 2011, **115**, 6057; J. Liu, T. Yang, D. Wang, G. Lu, D. Zhao, and S. Qiao, *Nat. Commun.*, 2013, **4**, 2798; W. Zhou, H. Chen, Y. Yu, D. Wang, Z. Cui, F. J. DiSalvo and H. D. Abruna, *ACS nano*, 2013, **7**, 8801; M. Q. Zhao, X. F. Liu, Q. Zhang, G. L. Tian, J. Q. Huang, W. Zhu and F. Wei, *ACS Nano*, 2012, **6**, 10759.
- 60 22 L. Suo, Y. Hu, H. Li, M. Armand & L. Chen, *Nat. Commun.*, 2013, **4**, 1481; Y. Cao, X. Li, I. A. Aksay, J. Lemmon, Z. M. Nie, Z. G. Yang, J. Liu, *Phys. Chem. Chem. Phys.*, 2011, **13**, 7660; D. Aurbach, I. Weissman, A. Zaban, Y. Ein-Eli, E. Mengeritsky and P. Dan, *J. Electrochem. Soc.*, 1996, **143**, 2110; L. Yuan, H. Yuan, X. Qiu, L. Chen and W. Zhu, *J. Power Sources*, 2009, **189**, 1141; X. Liang, Z. Wen, Y. Liu, H. Zhang, L. Huang and J. Jin, *J. Power Sources*, 2011, **196**, 3655.
- 70